Eur. Phys. J. D **42**, 341–348 (2007)
DOI: 10.1140/epjd/e2007-00049-1

THE EUROPEAN PHYSICAL JOURNAL D

Precision of single-qubit gates based on Raman transitions

X. Caillet and C. Simon[a]

Laboratoire de Spectrométrie Physique, CNRS, Université de Grenoble 1, St. Martin d'Hères, France

Received 30 January 2007
Published online 9 March 2007 –

Abstract. We analyze the achievable precision for single-qubit gates that are based on off-resonant Raman transitions between two near-degenerate ground states via a virtually excited state. In particular, we study the errors due to non-perfect adiabaticity and due to spontaneous emission from the excited state. For the case of non-adiabaticity, we calculate the error as a function of the dimensionless parameter $\chi = \Delta\tau$, where Δ is the detuning of the Raman beams and τ is the gate time. For the case of spontaneous emission, we give an analytical argument that the gate errors are approximately equal to $\Lambda\gamma/\Delta$, where Λ is the rotation angle of the one-qubit gate and γ is the spontaneous decay rate, and we show numerically that this estimate holds to good approximation.

PACS. 03.67.Lx Quantum computation – 73.21.La Quantum dots

QICS. 13.10.+n Effects of noise and imperfections – 15.10.Qd Quantum dots – 16.10.Es Electrons in semiconductors: spin

1 Introduction

The ability to perform arbitrary unitary transformations on individual qubits is very important in the context of quantum computation [1]. From the point of view of decoherence, it is often advantageous to use near-degenerate ground states of a given system as qubits, e.g. different hyperfine levels in a trapped ion or atom, or the spin states of an individual excess electron in a quantum dot. In such situations, the use of optical Raman transitions can be an attractive approach for realizing single-qubit operations, cf. reference [2] for experiments with trapped ions, reference [3] for a proposal involving atoms in an optical lattice, and reference [4] for a proposal with spins in quantum dots.

The use of Raman transitions is well-known also in the context of stimulated Raman adiabatic passage (STIRAP), which is commonly used for the coherent transfer of quantum states in atomic and molecular physics [5]. STIRAP has the advantages of eliminating the effects of spontaneous emission from the excited state entirely (because the system is always in a dark state) and of being robust with respect to fluctuations in the laser pulse area. However, for the classic STIRAP procedure the initial state of the system has to be known, whereas quantum gates have to work for arbitrary initial states. A scheme for single-qubit gates based on STIRAP has been proposed [6], which makes use of additional low-lying states. Unfortunately such states are not always available in a given physical system.

In particular, there are only two low-lying states in the case of a qubit realized by the two spin states of a single excess electron in a quantum dot, which is a very promising candidate system for the implementation of quantum computing. It is thus of interest to develop procedures for realizing arbitrary single-qubit operations via Raman transitions in such systems. Such a procedure has recently been proposed in reference [7]. The authors suggested to perform the Raman operation in an adiabatic fashion, in order to keep the population in the excited state as small as possible. In contrast to the case of STIRAP, the system does not remain in a dark state at all times, and the pulse area has to be precisely determined. Variations of the proposal involving different excited states of the quantum dots (light- hole excitons instead of heavy-hole excitons) were discussed in [8,9]. Let us note that there are several proposals on how to realize optically controlled two-qubit gates between individual spins in different quantum dots [4,8–10]. Schemes for qubit measurement have also been proposed [4,8,11].

Note that in the absence of spontaneous emission single-qubit operations could also be performed exactly in a non-adiabatic fashion via on-resonant Rabi rotations [12]. In the presence of spontaneous emission, the rotations have to be much faster than the spontaneous lifetime, to keep the emission probability from the excited state small. This typically requires very high laser intensities. Moreover, in the case of quantum dots, the interaction of the exciton with phonons also has to be taken into

[a] e-mail: chsimon@spectro.ujf-grenoble.fr

account [8,13]. This leads to large errors for fast operations, which however decrease very significantly for slower operations. The basic reason for this is that the speed of the operation determines the energy that is available for the creation of phonons (since the coupling is such that the system does not decay from the excited state during the phonon emission). The slower the operation, the less energy is available, restricting the available state space for the phonons. There is no corresponding energy constraint for spontaneous emission, since the energy for photon creation is provided by the decay of the emitter to one of the low-lying states. The combination of the two error mechanisms — emission of phonons and of photons — thus provides strong motivation for the use of the adiabatic protocol of reference [7], which promises to allow slower operations even in the presence of spontaneous emission.

In quantum computing, it is important to gain a detailed understanding of the expected size of the imperfections for any given quantum gate protocol. In reference [7] the authors briefly discussed the effects of non-perfect adiabaticity and of spontaneous emission from the excited state. In the present work we perform a more detailed study of these fundamental sources of error for the proposed gate protocol. In particular, we obtain quantitative results for the errors due to non-adiabaticity, and a simple formula for the errors due to spontaneous emission, namely that they are approximately equal to $\Lambda\gamma/\Delta$, where Λ is the rotation angle for the single-qubit rotation, γ is the spontaneous emission rate and Δ is the detuning of the two Raman lasers from the excited state. We give evidence for this result both with a simple formal argument and by numerical computation.

This paper is organized as follows. In Section 2 we describe the protocol for realizing arbitrary single-qubit gates via Raman transitions proposed in reference [7]. In Section 3 we study the errors due to non-perfect adiabaticity (in the absence of spontaneous emission). In Section 4 we study the errors caused by spontaneous emission. In Section 5 we give our conclusions.

2 Gate protocol

In this section we describe the gate protocol proposed in reference [7]. Consider a three level system composed of the two logical states of the qubit, $|0\rangle$ and $|1\rangle$, and an auxiliary excited state $|X\rangle$. The protocol relies on adiabatic Raman transitions in this Λ system, cf. Figure 1, using two phase-locked laser pulses. The two laser frequencies are chosen such that they have the same detuning Δ, i.e. they satisfy the Raman resonance condition.

The Hamiltonian in the interaction picture is:

$$H = \begin{pmatrix} 0 & 0 & \Omega_1(t)e^{i\alpha} \\ 0 & 0 & \Omega_2(t) \\ \Omega_1(t)e^{-i\alpha} & \Omega_2(t) & \Delta \end{pmatrix}, \tag{1}$$

where α is the relative phase between the two real Rabi frequencies $\Omega_1(t), \Omega_2(t)$. This Hamiltonian can be diagonalized straightforwardly. One introduces the following

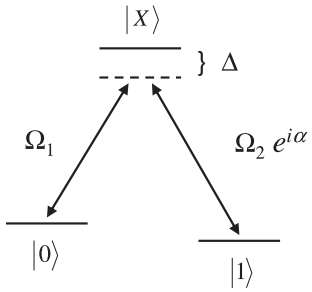

Fig. 1. Scheme for single qubit gates analyzed in this paper. The low lying states $|0\rangle$ and $|1\rangle$ serve as qubit states. They are coupled to an excited state $|X\rangle$ via two laser beams with time-dependent Rabi frequencies Ω_1 and $\Omega_2 e^{i\alpha}$. The laser beams have the same constant detuning Δ from the excited state.

parameters:

$$\Omega(t) = \sqrt{\Omega_1^2(t) + \Omega_2^2(t)} \tag{2}$$

$$Z(t) = \sqrt{\Omega^2(t) + \left(\frac{\Delta}{2}\right)^2} \tag{3}$$

$$\phi(t) = \frac{1}{2}\arctan\left(2\frac{\Omega(t)}{\Delta}\right) \tag{4}$$

$$\beta(t) = \arctan\left(\frac{\Omega_2(t)}{\Omega_1(t)}\right). \tag{5}$$

The angle β is maintained constant by choosing the same envelope shape for the two pulses. One obtains the eigenvalues:

- $\lambda_1(t) = 0$ with eigenvector

$$|\Phi_1(t)\rangle = \begin{pmatrix} -e^{i\alpha}\sin(\beta) \\ \cos(\beta) \\ 0 \end{pmatrix} \tag{6}$$

- $\lambda_2(t) = -2Z(t)\sin^2(\phi(t))$ with eigenvector

$$|\Phi_2(t)\rangle = \begin{pmatrix} -e^{i\alpha}\cos(\beta)\cos(\phi) \\ -\sin(\beta)\cos(\phi) \\ \sin(\phi) \end{pmatrix} \tag{7}$$

- $\lambda_3(t) = 2Z(t)\cos^2(\phi(t))$ with eigenvector

$$|\Phi_3(t)\rangle = \begin{pmatrix} e^{i\alpha}\cos(\beta)\sin(\phi) \\ \sin(\beta)\sin(\phi) \\ \cos(\phi) \end{pmatrix}. \tag{8}$$

The first eigenstate $|\Phi_1(t)\rangle$ is time independent and completely decoupled from the other two eigenstates. It has no contribution from the excited state $|X\rangle$. The second eigenstate $|\Phi_2(t)\rangle$ possesses only a small component of the excited state $|X\rangle$, as long as Ω/Δ is small. The last state $|\Phi_3(t)\rangle$ is mainly composed of the excited state $|X\rangle$.

An arbitrary unitary transformation can be realized adiabatically in the following way. Before the lasers are turned on (i.e. for $\phi = 0$), the initial qubit state can be

expressed as a linear combination of the first two eigenstates. By applying the two lasers, the Hamiltonian is then changed continuously. The adiabatic theorem states that, if the change of the Hamiltonian is sufficiently slow, the population in each instantaneous eigenstate remains constant, only the relative phases of the eigenstates change. In the subspace formed by the first two eigenstates, one obtains the following transformation:

$$[a, b] \longmapsto \left[a, be^{-i\Lambda_2}\right] \tag{9}$$

with

$$\Lambda_2 = \int_{t_i}^{t_f} \lambda_2(u)du, \tag{10}$$

where t_i and t_f denote the initial and final times respectively. From the point of view of the qubit basis spanned by the states $|0\rangle$ and $|1\rangle$, the resulting transformation has the form

$$U = e^{-i/2\Lambda_2 \vec{\sigma}\cdot\vec{n}}, \tag{11}$$

where $\vec{\sigma}$ is the vector of Pauli matrices, corresponding to a rotation through an angle Λ_2 about an axis described by a unit vector $\vec{n}$ with components

$$\begin{aligned} n_x &= \cos(\alpha)\sin(2\beta) \\ n_y &= -\sin(\alpha)\sin(2\beta) \\ n_z &= \cos(2\beta). \end{aligned} \tag{12}$$

We can now begin our detailed study of the corrections to this idealized description under realistic experimental conditions. We will start with errors due to non-perfect adiabaticity.

3 Errors due to non-adiabaticity

3.1 Exact equations of motion

The exact wave function can be expanded in terms of the previously defined instantaneous eigenstates, but with in general time-dependent coefficients:

$$\psi(t) = \sum_n a_n(t)\,|\Phi_n(t)\rangle \exp\left[-i\int_{t_i}^{t} \lambda_n(u)du\right]. \tag{13}$$

Writing out the Schrödinger equation for this wave function, one obtains the following evolution equations for the coefficients:

$$\begin{aligned} &\dot{a}_k \exp\left[-i\int_{t_i}^{t} \lambda_k(u)du\right] = \\ &\quad -\sum_n a_n(t)\langle\Phi_k(t)\|\dot{\Phi}_n(t)\rangle \exp\left[-i\int_{t_i}^{t} \lambda_n(u)du\right]. \end{aligned} \tag{14}$$

Substituting the values of the scalar products $\langle\Phi_i(t)\|\dot{\Phi}_j(t)\rangle$ according to the definition of the eigenstates, one finally has:

$$\begin{aligned} \dot{a}_1(t) &= 0 \\ \dot{a}_2(t) &= -\dot{\phi}(t)a_3(t)P_{23}(t) \\ \dot{a}_3(t) &= \dot{\phi}(t)a_2(t)P_{32}(t) \end{aligned} \tag{15}$$

with

$$\begin{aligned} P_{32}(t) = P_{23}^*(t) &= \exp\left(i\int_{t_i}^{t} (\lambda_3(v) - \lambda_2(v))\,dv\right) \\ &= \exp\left(2i\int_{t_i}^{t} Z(v)dv\right). \end{aligned} \tag{16}$$

The resolution of this system of differential equations allows to determine the error due to non-adiabaticity.

For a given desired transformation U, we will define the error as the maximum departure (in terms of overlap) of the real final state $\rho(t_f)$ from the ideal final state $|\psi_{ideal}\rangle = U|\psi(t_i)\rangle$, where the maximization is over all initial states:

$$E(U) = \max_{\psi(t_i)} \left[1 - \langle\psi_{ideal}|\,\rho(t_f)\,|\psi_{ideal}\rangle\right]. \tag{17}$$

The error can be expressed in terms of the complex coefficients $a_i(t_f)$. Since the coefficient a_1 always remains constant, $a_3(t_i) = 0$ and the differential equations are linear and homogeneous, it is in fact sufficient to solve the system of equations for one initial value of a_2, say $a_2(t_i) = 1$. The results for all possible initial states can then simply be obtained by multiplying the solution with the corresponding value of $a_2(t_i)$.

3.2 Calculation of the error due to non-adiabaticity

We now proceed to calculate the error due to non-perfect adiabaticity. To simplify the discussion, we will only consider laser pulse shapes $\Omega(t)$ that are approximate Gaussians of halfwidth τ centered at $t = 0$, slightly modified such that the Rabi frequency is exactly zero at the initial and final times (t_i and t_f). We introduce the ratio

$$x(t) = \frac{\Omega(t)}{\Delta} = x_{max} f(t), \tag{18}$$

where x_{max} is the maximal value of the ratio Ω/Δ, i.e. we have normalized f such that $f(0) = 1$. It should be pointed out that the considered gate protocol is advantageous only in the regime of relatively small $x(t)$. Using the protocol makes sense only when the excited state component in the adiabatic basis state $|\Phi_2(t)\rangle$ is small. According to equations (7) and (4), the squared excited state amplitude in $|\Phi_2(t)\rangle$ is given by

$$\sin^2\phi(t) = \frac{1}{2}\left(1 - \frac{1}{\sqrt{1 + 4x^2(t)}}\right). \tag{19}$$

For large values of x, the excited state components in the states $|\Phi_2\rangle$ and $|\Phi_3\rangle$ are approximately equal, and there is no reason to use the adiabatic gate protocol.

To show the role of the gate time more clearly, it is convenient to make the following substitutions. For each function g of the time t, we write $\tilde{g}(u) = g(\tau u)$, with the correspondence $t = \tau u$. Thus the new system evolves between the unitless time $u_i = t_i/\tau$ and $u_f = t_f/\tau$.

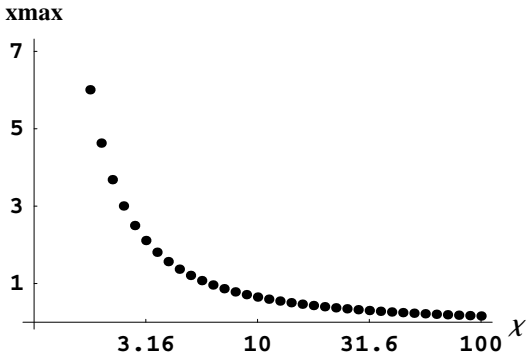

Fig. 2. Determination of x_{max}, the maximum value of the ratio Ω/Δ, as a function of the dimensionless parameter $\chi = \Delta\tau$ for a π rotation. The values for other rotation angles can be obtained from the fact that x_{max} depends only on the ratio χ/Λ.

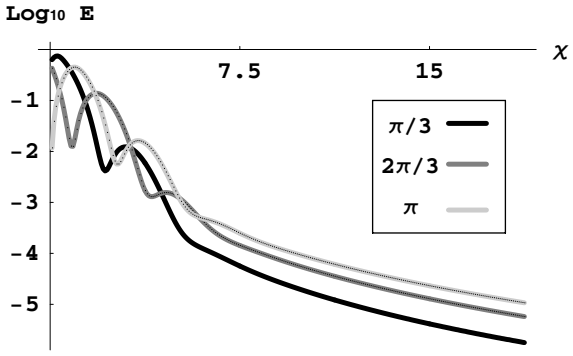

Fig. 3. Gate error as a function of χ for different rotation angles.

Introducing the dimensionless quantity

$$\chi = \Delta\tau, \tag{20}$$

i.e. the product of the detuning and the gate time, we obtain the functions

$$\tilde{P}_{32}(u) = \exp\left(-i\chi \int_{u_i}^{u} \sqrt{1 + 4x_{max}^2 \tilde{f}^2(v)}dv\right) \tag{21}$$

and

$$\dot{\tilde{\phi}}(u) = \frac{x_{max}\dot{\tilde{f}}(u)}{1 + 4x_{max}^2\tilde{f}^2(u)}, \tag{22}$$

which appear in the dimensionless evolution equations:

$$\dot{\tilde{a}}_2(u) = \dot{\tilde{\phi}}(u)\tilde{a}_3(u)\tilde{P}_{32}^*(u) \tag{23}$$

$$\dot{\tilde{a}}_3(u) = -\dot{\tilde{\phi}}(u)\tilde{a}_2(u)\tilde{P}_{32}(u). \tag{24}$$

We thus obtain a new system of differential equations depending on the two dimensionless parameters χ et x_{max}. In the following, we will study the gate error as a function of the rotation angle Λ and the dimensionless parameter χ. The quantity x_{max} is then not an independent variable, but is determined by these two parameters in the following way. After simplifications and substitutions, equation (10) becomes:

$$2\Lambda = \chi \int_{u_i}^{u_f} \left(\sqrt{1 + 4x_{max}^2\tilde{f}^2(u)} - 1\right) du = \chi g(x_{max}). \tag{25}$$

Recall that $\tilde{f}(u)$ is essentially a Gaussian with halfwidth 1 (apart from a small modification at the boundaries of the time interval), normalized such that its maximum value is equal to one. This equation gives x_{max} as an implicit function of the ratio Λ/χ. As g is an increasing function, and is a bijection from $[0, +\infty]$ to $[0, +\infty]$, we obtain a one to one correspondence between x_{max} and χ for a given Λ. Figure 2 shows that x_{max} is a decreasing function of χ. In the regime of small x_{max}, equation (25) can be simplified to

$$\Lambda = \chi x_{max}^2 \int_{u_i}^{u_f} \tilde{f}^2(u)du, \tag{26}$$

showing that x_{max} has to be of order $\sqrt{\Lambda/\chi}$ (since the integral is of order one). This explains the fact, clearly visible in Figure 2, that the regime of small x_{max} corresponds to the regime of large χ.

For a given rotation angle Λ, we finally obtain a system depending only on the parameter χ. By solving it numerically, we obtain an estimation of the adiabatic error as a function of χ and of Λ. Note that the error does not depend on the axis of rotation. Indeed, the choice of the axis of rotation only determines the relation of the basis of logical states to the basis of adiabatic eigenstates, and since the error is obtained by maximizing over all initial states, this choice has no effect on its value. The error as a function of χ for different values of the angle Λ is shown in Figure 3. For each value of Λ, we observe two characteristic regimes. The first one, where χ is small, is characterized by a damped oscillatory behaviour as a function of χ, leading also to a non-monotonous variation of the error with the rotation angle. In the second one, the error decreases continuously with χ, and greater values of Λ lead to larger errors.

The requirement of large χ can be understood qualitatively by considering equation (16). The coefficient a_3 will remain small as long as the phase factor $P_{32}(t)$ changes sign much faster than a_3 grows due to the factor $\dot{\phi}(t)$ (remember that a_2 can be taken to be equal to one at the beginning), i.e. as long as $\dot{\phi}(t) \ll Z(t)$, cf. reference [7]. In the regime of small Ω/Δ this can be rewritten as $\dot{\Omega}/\Delta \ll \Delta$. Approximating $\dot{\Omega}$ by Ω/τ one finds $\Delta\tau \gg \Omega/\Delta$. The exact results of Figure 3 show that a more accurate condition is $\chi = \Delta\tau \gg 1$, which is however not very different from the above estimate in the intermediate regime where Ω/Δ is smaller, but not much smaller than 1.

We briefly comment on the results for small χ, or equivalently large x_{max}, recalling that the considered protocol is not adapted to this regime. For large x_{max}, the phase ϕ approaches its maximum value of $\pi/4$ very quickly once the laser is turned on (and then stays approximately constant). As a consequence, one can convince oneself that a system starting out in one of the two low-lying states acquires a large component in the state $|\Phi_3\rangle$ almost immediately [12]. This leads to large errors in the framework of the present protocol, which assumes that

the population in $|\Phi_3\rangle$ remains very small. As mentioned above, precise gate operations in the on-resonant regime are possible in principle, in particular in the absence of other sources of error such as spontaneous emission of photons and phonons.

Our approach in this section has been partly numerical. Let us note that analytical techniques for calculating corrections to the adiabatic approximation have been developed and applied to problems such as STIRAP [14].

4 Errors due to spontaneous emission

4.1 Estimate of error based on population transfer

In this section we will investigate the error introduced to the Raman single-qubit gates by the finite lifetime of the excited state $|X\rangle$ due to spontaneous emission. We will begin with a fairly simple argument that gives the correct behaviour for the error, before presenting more precise numerical calculations in the next subsection.

As described before, the two adiabatic basis states that are significantly populated during the gate operation are $|\Phi_1(t)\rangle$ and $|\Phi_2(t)\rangle$. The state $|\Phi_1(t)\rangle$ has no contribution from the excited state and is thus unaffected by spontaneous emission. On the other hand, the state $|\Phi_2(t)\rangle$ has a component in the excited state $|X\rangle$. From equation (7), we can see that the population in the unstable state $|X\rangle$ is therefore $a_2^2(t)\sin^2(\phi(t))$. Defining γ as the spontaneous decay rate of the state $|X\rangle$, we can then estimate the population δ transferred by spontaneous emission during the gate operation as follows:

$$\delta = \int_{t_i}^{t_f} \gamma a_2^2(t)\sin^2(\phi(t))dt. \tag{27}$$

Let us assume that we are in the regime of small x_{max}, and that the overall error due to spontaneous emission is small, which implies that a_2 is nearly constant. Both assumptions will be well justified in any realization of the gate protocol that is relevant to quantum computation. Equation (27) can then be simplified to

$$\delta = \gamma\tau a_2^2 x_{max}^2 \int_{u_i}^{u_f} \tilde{f}^2(u)du, \tag{28}$$

where we have again introduced the dimensionless function $\tilde{f}(u)$ defined above. Comparing with equation (26), which is valid in the regime of small x_{max}, and choosing $a_2^2 = 1$ in order to obtain an upper bound, we find the following expression for the total transferred population due to spontaneous emission:

$$\delta = \Lambda\frac{\gamma}{\Delta}. \tag{29}$$

The error induced by spontaneous emission is twofold; on the one hand, a new distribution of the populations $\left|a_i^2\right|$, and on the other hand, a dephasing between the two qubit basis states. The transferred population δ provides an estimate for the gate error due to spontaneous emission. It may seem surprising that δ does not depend on the gate time τ, even though for longer gate times the component of the system in the excited state has more time to decay. The reason for this is that for the same rotation angle shorter gate times require larger populations in the excited state, and the two effects cancel out exactly, at least within the framework of the above estimate. We are now going to use numerical computation to obtain more precise results on the gate errors. Let us note that the effect of spontaneous decay on STIRAP was studied e.g. in reference [15].

4.2 Master equation

In order to study the effects of spontaneous emission on the Raman gate protocol in detail, we use the master equation formalism. In the present section, we assume for simplicity that the spontaneous emission can only occur from the state $|X\rangle$ toward the two qubit states $|0\rangle$ and $|1\rangle$, and not to any additional states. To take this decay into account, we introduce the Lindblad operators:

$$L_i = \sqrt{\gamma_i}\sigma_i \tag{30}$$

with $\sigma_i = |i\rangle\langle X|$ (for $i = 0, 1$). The constants γ_i are the decay rates from $|X\rangle$ towards the states $|i\rangle$. The total decay rate is thus given by $\gamma = \gamma_1 + \gamma_2$.

The master equation [1] is:

$$\frac{d\rho}{dt} = -i\left[H,\rho\right] + \sum_i \left(2L_i\rho L_i^+ - \left\{L_i^+ L_i, \rho\right\}\right). \tag{31}$$

For quantum gate operations, the initial state $|\psi\rangle$ is always a linear combination of the two logical states $a|0\rangle + b|1\rangle$ with $|a|^2 + |b|^2 = 1$.

The master equation corresponds to a set of coupled differential equations for the elements of the density matrix that can be solved numerically. This allows us to determine the gate error defined in equation (17).

4.3 Example — populations and purity

In this subsection, we describe the numerical results for a particular case in detail, comparing the situations with and without spontaneous emission. This is intended to serve as an introduction and illustration for our more general results presented in the next subsection.

We consider a rotation by π along the x-axis, corresponding to $\alpha = 0$ and $\beta = \pi/4$. The initial state of the system is the state $|0\rangle$. The ideal final state is the state $|1\rangle$. We choose the values $\tau = 0.01$ ns, $\Delta = 1$ meV $\approx 1500\ \text{ns}^{-1}$ and $\gamma_1 = \gamma_2 = 20\ \text{ns}^{-1}$. While these values could apply to conceivable experiments with quantum dots [16], we have also chosen them such that the relevant effects are clearly visible. For these values $\chi = 15$. The adiabatic approximation is thus very well satisfied, cf. Figure 3.

Figure 4a shows the time evolution of the populations in the states $|0\rangle$, $|1\rangle$ and $|X\rangle$ without spontaneous

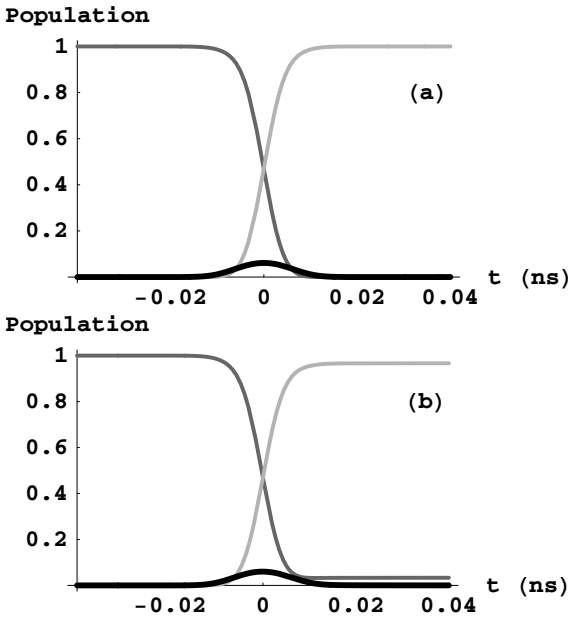

Fig. 4. Evolution of the populations during a π rotation of the state $|0\rangle$ around the x-axis into the state $|1\rangle$: (a) without spontaneous emission; (b) with spontaneous emission.

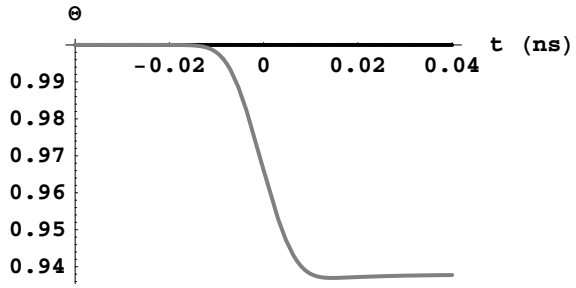

Fig. 5. Evolution of the purity of the state, $\Theta(t)$, without and with spontaneous emission.

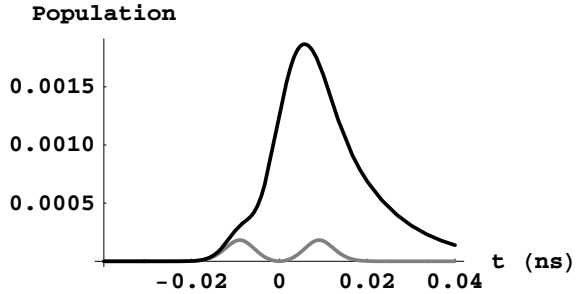

Fig. 6. Time evolution of the population in the adiabatic basis state $|\Phi_3(t)\rangle$ (whose dominant component is in the excited state $|X\rangle$) without and with spontaneous emission.

emission. As expected, the populations in the states $|0\rangle$ and $|1\rangle$ are exchanged. Moreover, the population in $|X\rangle$ is zero at the end of the operation. One can describe the evolution of the system in detail as follows. The initial state $|0\rangle$ can be expressed in the adiabatic basis as:

$$|0\rangle = -\frac{1}{\sqrt{2}}\left(|\Phi_1(t_i)\rangle + |\Phi_2(t_i)\rangle\right). \tag{32}$$

The final state $|1\rangle$ can be written:

$$|1\rangle = \frac{1}{\sqrt{2}}\left(|\Phi_1(t_f)\rangle - |\Phi_2(t_f)\rangle\right) \tag{33}$$

with $|\Phi_1(t_f)\rangle = |\Phi_1(t_i)\rangle$ and $|\Phi_2(t_f)\rangle = |\Phi_2(t_i)\rangle$. The transformation is adiabatic: expressed in the basis $(|\Phi_1(t)\rangle,|\Phi_2(t)\rangle)$, the state of the system is:

$$|\Phi(t)\rangle = -\frac{1}{\sqrt{2}}[1, e^{i\Lambda(t)}]. \tag{34}$$

While the lasers are on, the phase $\Lambda(t)$ grows and thus the state $|0\rangle$ is continuously transformed into the state $|1\rangle$. The state $|\Phi_2(t)\rangle$ has a component of order $x_{max}f(t)$ in the state $|X\rangle$, the population in the excited state therefore grows until the maximum of the light intensity is reached, and then returns to zero. Figure 4b shows the same populations in the presence of spontaneous emission. It appears clearly that the rotation is no longer perfect in this case. The populations in the initial state $|0\rangle$ and in the excited state $|X\rangle$ are no longer zero at the moment when the light is turned off. Of course the remaining population in $|X\rangle$ will decay towards the states $|0\rangle$ and $|1\rangle$ on the larger timescale set by $\gamma_{1,2}$.

The departure from the perfect rotation can be further visualized by analyzing the purity of the system density matrix $\rho(t)$, i.e. by studying the quantity $\Theta(t) = \mathrm{Tr}\rho(t)^2$. Figure 5 shows the evolution of Θ with and without spontaneous emission. As expected, Θ remains constant in the absence of spontaneous emission. In the presence of spontaneous emission, the purity decreases considerably. This decrease is particularly strong around $t = 0$, i.e. around the maximum of the laser intensity. It is at this point that the population in the state $|X\rangle$ becomes the largest. The spontaneous emission from $|X\rangle$ causes the state to become mixed.

Figure 6 shows the time evolution of the population in the state $|\Phi_3(t)\rangle$ of equation (8). One sees that in the absence of spontaneous emission the adiabatic approximation is well justified, the population in the state remains very small. Its departure from zero corresponds to the error due to non-perfect adiabaticity discussed in the previous section. On the other hand, the presence of spontaneous emission causes transitions between the states $|\Phi_2(t)\rangle$ and $|\Phi_3(t)\rangle$, which populate the latter. This population decreases on the timescale of the radiative lifetime, since $|\Phi_3(t)\rangle$ contains predominantly the excited state $|X\rangle$.

4.4 General results on errors due to spontaneous emission

In this subsection we will present more general results on the error due to spontaneous emission. In particular we want to test the estimate made in Section 4.1. Figure 7 shows the error for a rotation by π as a function of the gate time τ in the presence of a spontaneous emission. This graph should be compared to Figure 3, which shows

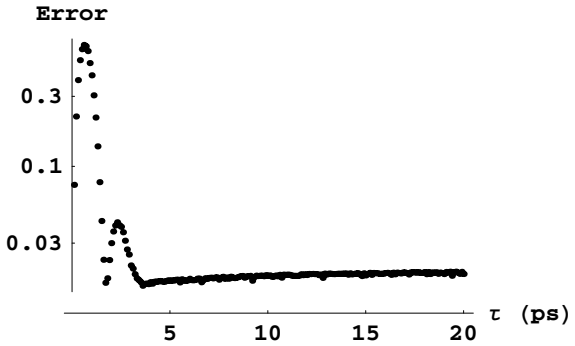

Fig. 7. Gate error in the presence of spontaneous emission as a function of the gate time τ. The spontaneous decay rates are $\gamma_1 = \gamma_2 = 5$ ns^{-1}, the detuning $\Delta = 1$ meV. The variation of τ between 0 and 20 ps corresponds to the dimensionless parameter $\chi = \Delta\tau$ varying from 0 to 30.

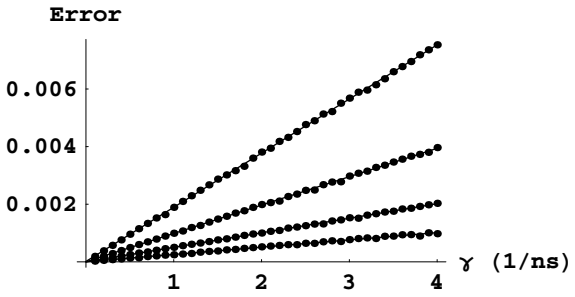

Fig. 8. Gate error for a π rotation as a function of the spontaneous decay rate γ for fixed values of the detuning $\Delta = 1, 2, 4, 8$ meV respectively (from top to bottom graph).

the same quantity in the absence of spontaneous emission. For short times the behaviour is very similar, showing the same damped oscillatory character. In this regime, the error is dominated by non-perfect adiabaticity. For longer gate times, there is a clear difference. In the presence of spontaneous emission, the error does not fall below a certain minimal value and is virtually independent of τ. This is in good correspondence with the prediction made in Section 4.1.

In order to test the above estimate more systematically, we have performed calculations varying γ and Δ for a fixed value of the gate time $\tau = 13.3$ ps. We restrict ourselves to values of $\Delta \geq 1$ meV, corresponding to $\chi \geq 20$, in order to make sure that the error due to non-adiabaticity is negligible, cf. Figure 3. Furthermore we focus on the regime where the overall gate error is at most at the percent level, since this is the relevant regime for quantum computing. The total spontaneous decay rate is $\gamma = \gamma_1 + \gamma_2$. For simplicity we have again chosen $\gamma_1 = \gamma_2$.

Figure 8 shows the behaviour of the gate error of a π rotation as a function of the spontaneous decay rate γ for four different values of the detuning Δ. One sees that the error is linear in γ with a high degree of accuracy. Similarly, Figure 9 shows the gate error as a function of Δ for three different values of γ. One sees that the results are fitted extremely well by a $1/\Delta$ behaviour. The proportionality of the error to γ/Δ is thus seen to be very well

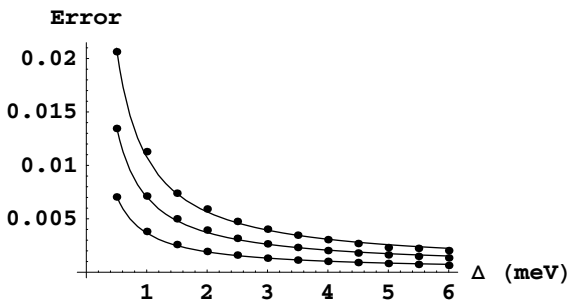

Fig. 9. Gate error of a π rotation as a function of detuning Δ for fixed values of the spontaneous decay rate $\gamma = 2, 4, 6$ ns^{-1} respectively (from bottom to top graph). The curves are fits to a $1/\Delta$ behaviour.

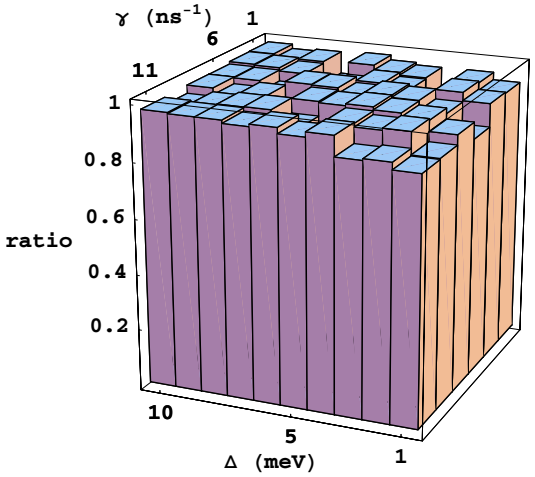

Fig. 10. Ratio of the (numerically obtained) exact value of the error for a π rotation to the value of $\pi\gamma/\Delta$ given by the estimate of Section 4.1 for a range of values of γ and Δ.

obeyed. To assess the accuracy of the above estimate concerning the absolute size of the error, Figure 10 compares the errors obtained numerically for a π rotation to the estimated error of $\pi\gamma/\Delta$. One sees that the approximation works very well in the considered regime. As expected, it tends to work somewhat less well for increasing values of γ and decreasing values of Δ, i.e. increasing overall size of the error, cf. Section 4.1.

5 Conclusions

The results obtained in the present paper give quantitative information for the implementation of quantum gates using the protocol of reference [7]. The results of Section 3 on the errors due to non-perfect adiabaticity give the necessary conditions on gate speed, detuning and laser intensity for any desired level of error. The results of Section 4 quantify the errors due to spontaneous emission, whose presence is unavoidable for the studied gate protocol. In the context of quantum computing with spins in quantum dots, the present analysis complements the results of references [8,13] on quantum gate errors due to

phonon-induced dephasing. As discussed in the introduction, phonon-related errors can be made small by slowing down the gate operation. Our analysis shows that it is possible to choose relatively long gate times even in the presence of spontaneous emission, without significantly changing the size of the error due to the decay. Of course, the gate time always has to be much shorter than the decoherence time of superpositions of the qubit states.

We are grateful to J. Eymery, J.-M. Gérard, Y.-M. Niquet and J.-P. Poizat for useful discussions.

References

1. M.A. Nielsen, I.L. Chuang, *Quantum Computation and Quantum Information* (Cambridge University Press, Cambridge, 2000)
2. C. Monroe, D.M. Meekhof, B.E. King, W.M. Itano, D.J. Wineland, Phys. Rev. Lett. **75**, 4714 (1995); M.A. Rowe et al., Nature **409**, 791 (2001)
3. G.K. Brennen, C.M. Caves, P.S. Jessen, I.H. Deutsch, Phys. Rev. Lett. **82**, 1060 (1999)
4. A. Imamoglu et al., Phys. Rev. Lett. **83**, 4204 (1999)
5. K. Bergmann, H. Theuer, B.W. Shore, Rev. Mod. Phys. **70**, 1003 (1998)
6. Z. Kis, F. Renzoni, Phys. Rev. A **65**, 032318 (2002)
7. P. Chen, C. Piermarocchi, L.J. Sham, D. Gammon, D.G. Steel, Phys. Rev. B **69**, 075320 (2004)
8. T. Calarco, A. Datta, P. Fedichev, E. Pazy, P. Zoller, Phys. Rev. A **68**, 012310 (2003)
9. A. Nazir, B.W. Lovett, S.D. Barrett, T.P. Spiller, G.A.D. Briggs, Phys. Rev. Lett. **93**, 150502 (2004)
10. C. Piermarocchi, P. Chen, L.J. Sham, D.G. Steel, Phys. Rev. Lett. **89**, 167402 (2002)
11. R.-B. Liu, W. Yao, L.J. Sham, Phys. Rev. B **72**, 081306(R) (2005)
12. Z. Kis, E. Paspalakis, Phys. Rev. B **69**, 024510 (2004)
13. K. Roszak, A. Grodecka, P. Machnikowski, T. Kuhn, Phys. Rev. B **71**, 195333 (2005)
14. M.V. Berry, Proc. Roy. Soc. Lond. A **429**, 61 (1990); M. Elk, Phys. Rev. A **52**, 4017 (1995); K. Drese, M. Holthaus, Eur. Phys. J. D **3**, 73 (1998); S. Guérin, S. Thomas, H.R. Jauslin, Phys. Rev. A **65**, 023409 (2002)
15. N.V. Vitanov, S. Stenholm, Phys. Rev. A **56**, 1463 (1997)
16. T. Flissikowski et al., Phys. Rev. Lett. **86**, 3172 (2001); E. Moreau et al., Phys. Rev. Lett. **87**, 183601 (2001); D. Gammon, E.S. Snow, B.V. Shanabrook, D.S. Katzer, D. Park, Science **273**, 87 (1996)